

Supporting Information

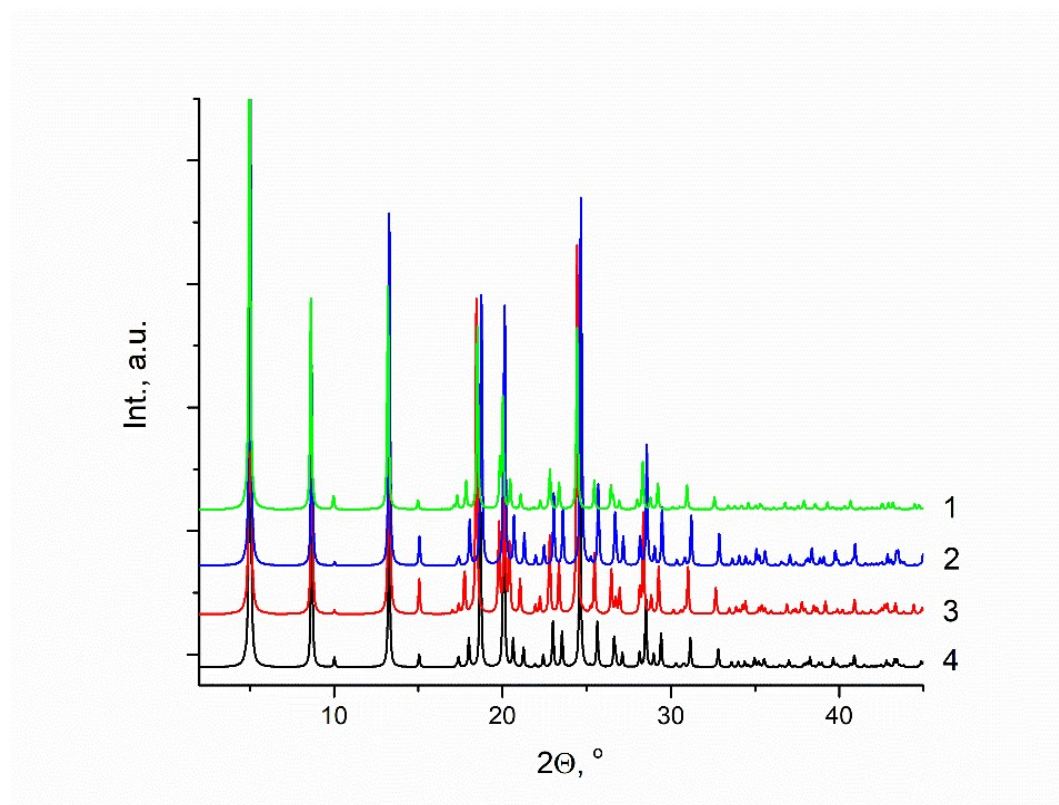


Fig. S1 Theoretical powder diffraction patterns generated from single-crystal X-ray diffraction data for CBZ(II) (1, CCDC number 1121423) [M. M. J. Lowes, M. R. Caira, A. P. Lötter and J. G. Van Der Watt, *J Pharm Sci*, 1987, **76**, 744–752], CBZ : 0.33H₂O hydrate (2, CCDC number 905203) [R. Prohens, M. Font-Bardia and R. Barbas, *CrystEngComm*, 2013, **15**, 845–847], CBZ : 0.17H₂O hydrate (3, CCDC number 1494538) [P. P. Nievergelt and B. Spingler, *CrystEngComm*, 2017, **19**, 142–147] and solvate CBZ with THF (4, CCDC number 641710) [F. P. A. Fabbiani, L. T. Byrne, J. J. McKinnon and M. A. Spackman, *CrystEngComm*, 2007, **9**, 728–731].

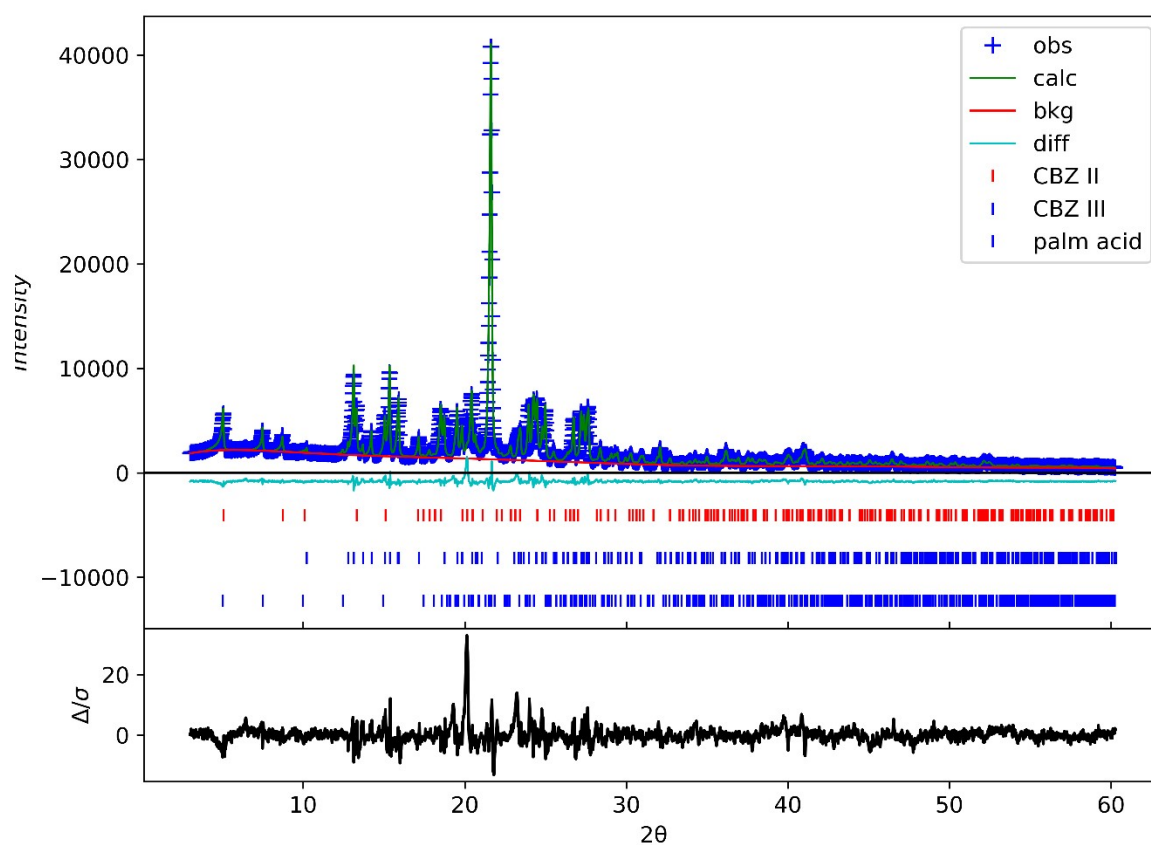


Fig. S2 Rietveld refinement plot for experiment on dissolution of CBZ (III) in palmitic acid and its recrystallization into CBZ (II) (Fig. 3a, exp. 1 in the main text). $R=4.21\%$, $wR=6.43\%$. Qualitative composition (weight fraction): palmitic acid – 48%, CBZ (III) – 37% CBZ (II) – 15%.

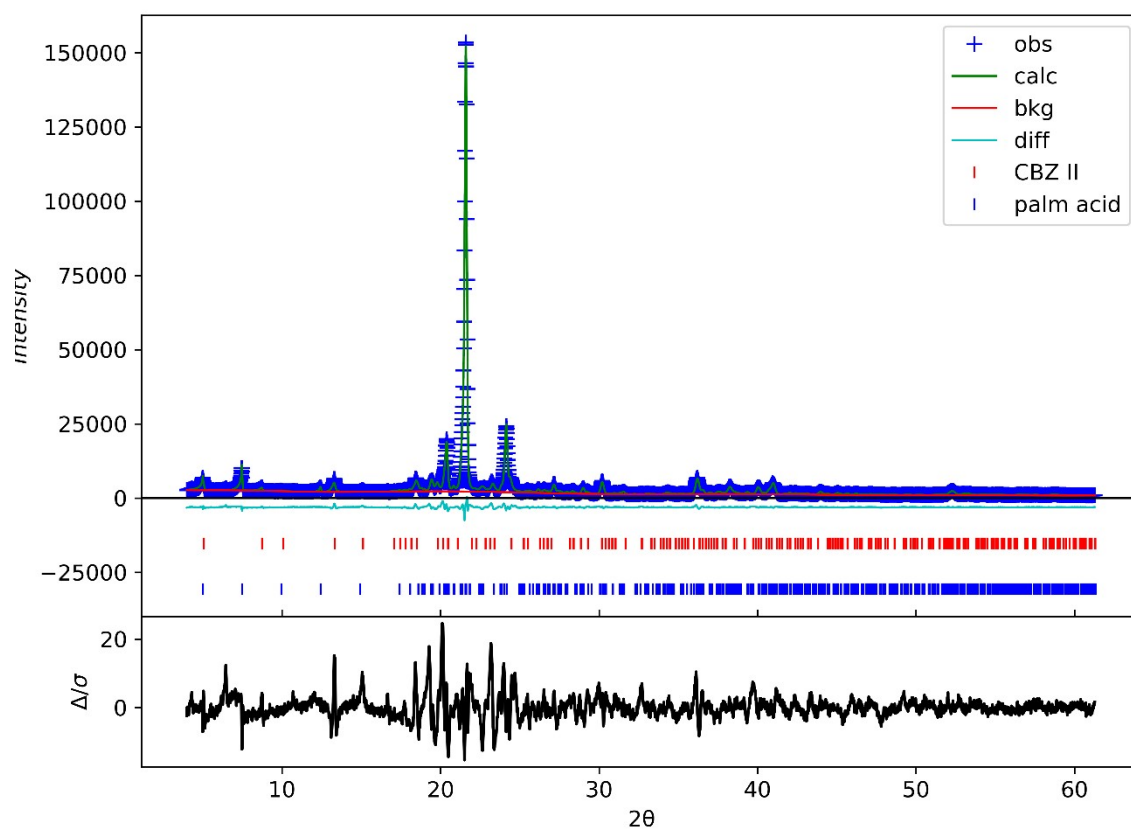


Fig. S3 Rietveld refinement plot for experiment on dissolution of CBZ (III) in palmitic acid and its recrystallization into CBZ (II) (Fig. 3b, exp. 2 in the main text). $R=4.30\%$, $wR=6.11\%$. Qualitative composition (weight fraction): palmitic acid – 96%, CBZ (II) – 4%.

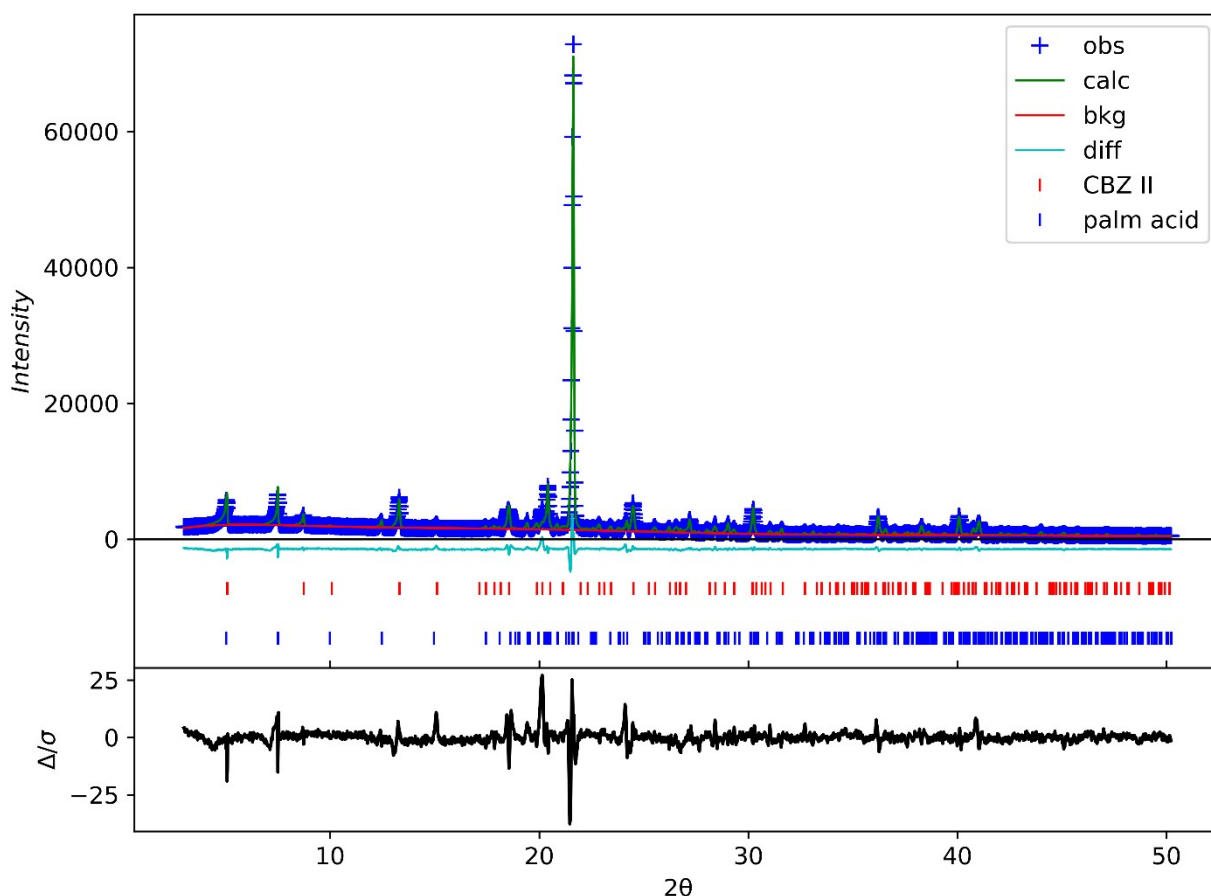


Fig. S4 Rietveld refinement plot for experiment on dissolution of CBZ (III) in palmitic acid and its recrystallization into CBZ (II) (exp. 3 in the main text). $R=5.06\%$, $wR=7.72\%$. Qualitative composition (weight fraction): palmitic acid – 88%, CBZ (II) – 12%.

Rietveld refinement was performed in GSAS II programme [Toby, B. H., & Von Dreele, R. B. (2013). GSAS-II: the genesis of a modern open-source all-purpose crystallography software package. *Journal of Applied Crystallography*, 46(2), 544-549]. Multiple model parameters were refined against experimentally observed data by Rietveld method. Background function and sample displacement parameters were refined at first step. Then unit cell parameters, phase fractions, micro-strain and domain sizes of individual phases were refined. Preferred orientation was treated in spherical harmonic model at final step.